

COMPARATIVE RISK ESTIMATION OF COMPRESSED HYDROGEN AND CNG REFUELLING OPTIONS

A. Tchouvelev¹, R. Hay² and P. Benard³

1. Introduction

This paper discusses the key results of the *Comparative Quantitative Risk Estimation of Hydrogen and CNG Refuelling Options* project [1] conducted within the Canadian Hydrogen Safety Program for the Codes & Standards Working Group of the Canadian Transportation Fuel Cell Alliance. The project comprised a comprehensive analysis of several hydrogen sourcing and refueling site configurations of which only a few representative examples of the analysis are described in this paper due to space limitations.

Engineering analysis and public perception of risk require both quantitative and qualitative assessments to assist in design and public acceptance of hydrogen refuelling stations. Quantitative risk assessment methodologies were applied to several safety-critical issues in hydrogen refuelling stations to generate design criteria and metrics for codes and standards development. To position the hydrogen station within the risk aversion perspective of the general public, these analyses were carried out in parallel with corresponding analyses for CNG (methane) stations. The latter represent consumer facilities where a public risk aversion level has been established and provides a reference with which risk analysis can be conveyed on a cooperative basis.

The risks analyses in the project are those associated with unintentional releases of hydrogen. Twelve such release scenarios were considered through the hydrogen life cycle from sourcing at the station to the dispenser. Sourcing options included delivery by tube trailer and on-site generation by electrolysis and hydrocarbon reforming.

The release scenarios selected were based on a composite of the literature-based and in-house hazard identification analyses. They are a series of safety-critical issues that represent those concerns that provide key input to design and public acceptance decision making.

A two-fold risk analysis approach comprised determining the *probability* of the releases in each scenario developing and *consequence modeling*, the latter including analysis of the dispersion of hydrogen under the scenario release conditions and the consequences of ignition of the hydrogen. The probability component was computed

¹ A.V.Tchouvelev & Associates Inc., 6591 Spinnaker Circle, Mississauga, ON Canada L5W 1R2

² Tisec Inc., 2755 Pitfield Boulevard, Montreal, QC Canada H4S 1T2

³ Hydrogen Research Institute, Université du Québec à Trois-Rivières, 3351 Boulevard des Forges, CP 500, Trois-Rivières, QC Canada G9A 5H7

using failure-rate data from the CTFCA database as input to fault and event tree analysis. The thermal consequence models provided a set of radiant heat fluxes expressed in kW/m^2 at a set of distances at which the following heat flux thresholds occurred:

4.7 kW/m^2	A pain threshold
12.5 kW/m^2	First-degree burn threshold
37.5 kW/m^2	Mortality threshold

Each scenario is addressed via a table that contains a diagram with distances to selected thermal threshold levels. The diagrams show maximum values for each threshold level in radial direction, i.e. outside the jet flame. Because of different intensity of releases in selected scenarios, the maximum values are achieved at different axial distances from the point of release. In order to compare thermal effects at equal distances from the points of release and resulting jet fires, the tables also contain the numbers for locations 1 m and 5 m away from the point of release in axial direction and 1 m in radial direction. They are marked $(x, R) = (1 \text{ m}, 1 \text{ m})$ and $(x, R) = (5 \text{ m}, 1 \text{ m})$ respectively. The values of thermal effects at these locations are used for risk calculations in Risk Estimation section of this report. For cases when selected locations are within the flame (i.e. thermal flux is much greater than 37.5 kW/m^2), the fatality probability is considered to be equal to 1.

Each of these distinct pairs of radiant heat flux and distances from the origin of the hazard was transformed into a probability of fatality at that specific distance, a consequence metric to be used for computation of risk. This transformation was performed using the Probit Equation (dose-response relationship).

Metrics were adopted to quantify the individual and societal risks associated with the scenarios analyzed in this project to effect comparisons between selected hydrogen sourcing, storage and hydrogen production components in hydrogen refuelling options. These were computed using HyQuantrasTM, a computerized toolkit for quantifying the risk associated with the jet-fire and flare scenarios used for these comparisons. Location-Specific Individual Risk (LSIR) and Potential Loss of Life (PLL) were used for the project comparisons.

The project data were used to compare various sourcing for hydrogen:

- Tube trailer delivery
- On-site production by electrolysis
- On-site production by reforming

and to compare the risk associated with storage modes of the two fuels. Also, the delivery of hydrogen by tube trailer and of natural gas through pipeline was compared.

2. TIAX FMEA Study

In 2005 TIAX released an FMEA study of the hydrogen refuelling option compared to a CNG refuelling option [2]. This TIAX study provides good qualitative guidance regarding the comparative risk of various hydrogen technologies vs CNG technology as well as regarding potential “stand-out” scenarios for more detailed modeling. The current study extends beyond the comparison at the qualitative FMEA level detailed quantitative comparison of “stand-out” elements that are either technology or fuel related. With the permission of TIAX, their FMEA approach and risk factors for various hydrogen technologies-based refuelling options in comparison with a CNG refuelling option are summarized below. The latter was chosen based on operation of CNG refuelling at UC Davis.

TIAX used a three-point scale of **low (L)**, **medium (M)**, and **high (H)** to rank both the **frequency** of occurrence (**F**) of the failure mode and the **consequence** of the failure mode (**C**) frequency and consequence for determining the relative risk of potential failures. This Frequency and Consequence rating scheme is presented in the Table 1.

Table 1 TIAX FMEA frequency and consequence rating scheme

Frequency Rating	Description
High (H)	Almost certain to occur repeatedly
Medium (M)	Likely to occur to rarely likely to occur
Low (L)	Unlikely that failure would occur

Consequence Rating	Description
High (H)	Potential for great harm or death if someone is present within the impact area.
Medium (M)	Harm would require some medical treatment to some pain or discomfort if someone is present within the impact area
Low (L)	End user, if present, would not notice

The consequence and frequency ratings for each FMEA are combined in the risk-binning matrix to estimate risk. Each hazard is plotted on a frequency vs. consequence matrix that yields an estimate of risk as high, moderate, low, or negligible. High risks are considered combinations of M x H, H x M, and H x H ratings. Moderate risks are combinations of L x H, H x L, and M x M. Finally low risks are combinations of L x M, M x L, L x L, and no safety hazard or negligible risk scenarios.

Using this approach, TIAX developed binning matrices for the three hydrogen options and a CNG option **Error! Reference source not found..**

This qualitative risk analysis by TIAX highlighted the following important conclusions:

- None of the hydrogen refuelling options considered presented high risk and generally all the hydrogen refuelling options considered were at par with a CNG refuelling option;
- In terms of medium risk, CNG refuelling presents less risk due to the simplicity of the system and generally lower pressure;
- In terms of medium risk, reformer technology is marginally riskier due to higher complexity arising from the need to deal with two fuels, methane and hydrogen, a higher process temperature and a higher internal inventory of gases;
- Electrolyser-based and tube trailer options are approximately at par in terms of medium risk.

Some of the scenarios considered by TIAX in the FMEA analysis were identified as “stand-outs” and were used for this project. They are identified in Section **Error! Reference source not found..**

3. Refuelling Station Design Basis

An existing CNG refuelling station was taken as a basis for design comparison of all 4 refuelling options. Table 2 below presents the design basis selected for the QRA.

The refuelling capacity is based on filling ten (10) hydrogen or CNG vehicles per day. Table 2 shows how the fuel fill rates reflect vehicle fuel economy and driving assumptions.

Table 2 Fuel fill rates reflected in vehicle fuel economy and driving assumptions

Refueling Station Common Design Bases

	Hydrogen	CNG
Number of vehicles refueled	10 per day	
Amount of fuel per fill	3 kg (1270 scf)	15.4 kg (743 scf)
Driving per fill	185 km (115 miles)	
Vehicle refueling time	10 min/fill	
Station average consumption	30 kg/day	7430 scf/day
Nominal dispensing capacity	5 vehicles in 2 hours	
Typical fuel consumption (gasoline equivalent)	4 L/100 km (60 mpg)	7.9 L/100 km (30 mpg)

The assumed energy consumption (in Btu/mile) of the CNG vehicles is roughly twice that of an identical hydrogen fuel cell vehicle. The relationship between CNG and

hydrogen vehicle energy consumption would be different for dissimilar vehicles or power plant configurations.

4. Scenario Definition

The following scenarios were selected after detailed review of available HazOPs and FMEA analysis, including TIAX report:

Table 3 Stand-out failure scenarios

Technology	Scenario Description / Details
Tube Trailers	<ol style="list-style-type: none"> 1. Small size leak (1 mm) on a ½” pipe line during unloading. Pressure – 2,640 psig, leak direction – horizontal; type of release – sonic jet. Mode of release – steady state, constant flow. 2. Catastrophic failure hydrogen release from ½” pipe line during unloading. Details similar to above. Mode of release – transient, exponentially changing flow. Hydrogen quantity – 370 kg.
Electrolysis	<ol style="list-style-type: none"> 3. Catastrophic failure hydrogen release from hydrogen rinser inside the electrolyser cabinet. Pressure – 10 bars; leak orifice – ¾” pipe; leak direction – horizontal; type of release – sonic jet. Hydrogen quantity – about 0.5 Nm³. Mode of release – transient. 4. Venting of released hydrogen from scenario 3 through the exhaust fan from the generator to atmosphere. Mode of release – transient. 5. Hydrogen line leak downstream of compressor towards storage outdoors. Pressure – 6,000 psig; effective leak orifice – 1 mm on a 3/8” tubing. Line flow rate – 1.25 kg/h. Type – sonic; mode – steady state. (This scenario will apply to reformer technology as well).
Reformer	<ol style="list-style-type: none"> 6. Natural gas supply line leak outdoors. Line pressure – 5 psig; leak size ¼” effective diameter on a ¾” pipe. Side leak at the ground level; steady state. 7. Natural gas line leak downstream of compressor towards reformer. Line pressure 150 psig (10 bars); effective leak orifice – 1 mm on a 3/8” tubing. Full flow in the line – 5.04 kg/h. 8. Catastrophic failure hydrogen release inside enclosure due to failure of the line between PSA unit and compressor. Line pressure – 10 bars; leak orifice – ½”. Mode – transient to release hydrogen contained in six PSA units and a surge tank. Type of release – sonic.
CNG Station	<ol style="list-style-type: none"> 9. Natural gas supply line leak outdoors. Line pressure – 5 psig; leak size ¼” effective diameter on a ¾” pipe. Side leak at the ground level; steady state. 10. Natural gas line leak downstream of compressor towards storage. Pressure – 4,000 psig; effective leak orifice – 1 mm on a 3/8” tubing. Line full flow rate – 18 kg/h; leak direction – horizontal, towards storage; Type – sonic; mode – steady state. Leak location: 4 ft from storage and 2 ft above ground level. See diagram Fig. 4-

	17 of TIAX FMEA report.
Gas Storage	<p>11. Hydrogen and CNG similar catastrophic type leaks through a ½” orifices from a 3-cylinder bank at 4,100 psig. Type – sonic; mode – transient; leak direction – horizontal.</p> <p>12. Venting of hydrogen and CNG through the same vent stack at 2,000 CFM flow rate. Type – sonic and subsonic; mode – steady state.</p>

5. Source Modeling

Due to limited size of the paper only most significant results in terms of sizes of resulting hydrogen clouds are being discussed here, namely tube trailer scenarios (small and large leaks for comparison) and both hydrogen and CNG ground storage.

5.1. Tube Trailer Failure Scenarios

Tube trailers are generally used to economically transport large quantities of compressed hydrogen. A typical hydrogen steel tube trailer contains several high-pressure cylinders for hydrogen storage, as shown in Figure 1.



Figure 1. A typical steel tube trailer for transportation of fuel gases

As per adopted modeling scenarios, the task was to simulate an effect of potential hydrogen releases by evaluating the LFL hydrogen cloud caused by leaks from the high-pressure cylinders. It is assumed that the initial release pressure is 2640 psig (182 bars). The CFD modeling of hydrogen releases and dispersion is used for the failure scenarios that consider the following conditions:

- 1) Small size leak (1 mm leak orifice) on a ½” pipe line during unloading. The stagnation pressure inside the cylinders is 2640 psi. Leak direction is horizontal and is perpendicular to the central line of the cylinders. Due to the high leak pressure, the leak is choked (sonic jet release).
- 2) Catastrophic failure hydrogen release from ½” pipe line during unloading. It is estimated that the internal diameter for the leak orifice is 8.48 mm. The pressure

inside the cylinders is 2640 psi. The leak direction is horizontal and parallel to the central line of the cylinders. It is a sonic jet release.

Figure 2 shows the two modeling scenarios for the current task. We assume that the total cylinder water volumes are large enough, and therefore, the mode of release can be simplified as a steady state and a constant flow.

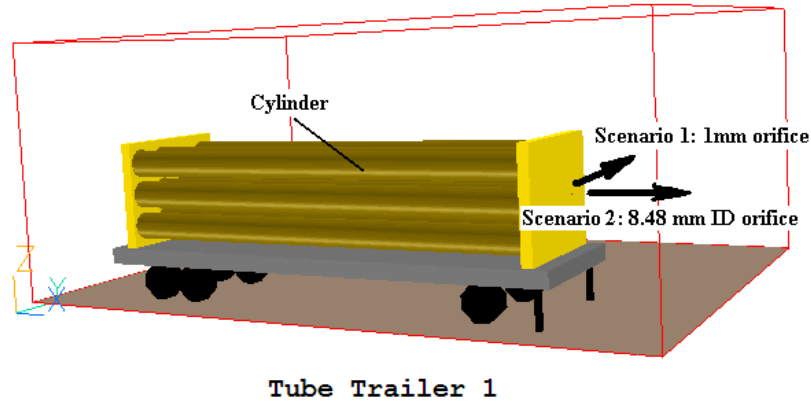


Figure 2. Modeling scenarios for the tube trailer.

Numerical Results

Scenario 1:

Horizontal hydrogen release from the 1 mm orifice was simulated using a domain size of 12.5 m long by 9 m wide by 5 m high with a grid size of 34×23×29. The compressible CFD models exploited the real gas law implemented by the Abel—Noble Equation of State and the LVEL turbulent models for the steady state simulation. Figure 3 shows the numerical results for the hydrogen concentration distribution along the leak direction. The LFL hydrogen cloud extent is about 4.26 m long from the leak orifice in the horizontal direction.

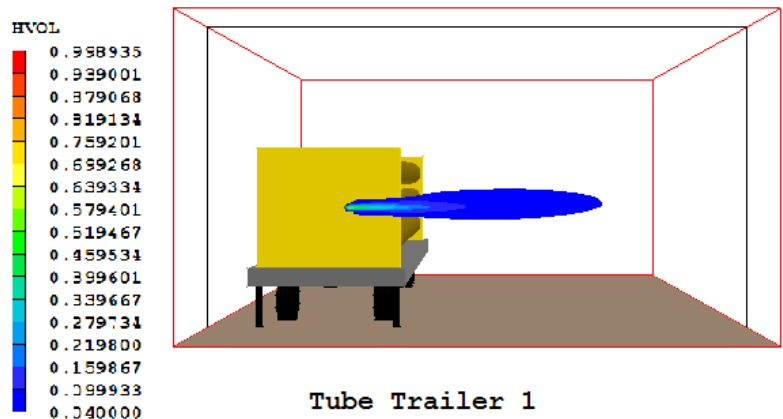


Figure 1. Hydrogen concentration distribution along the leak direction (Front view).

Scenario 2:

Horizontal hydrogen release from 8.48 mm ID orifice was simulated using a domain size of 70 m long by 12 m wide by 15 m high with a grid size of 29×26×27. The real gas law represented by the Abel—Noble Equation of State was implemented into the compressible CFD models. Figure 4 shows the numerical results for the LFL hydrogen cloud along the leak direction. The maximal horizontal cloud extent is about 40.5 m from the leak orifice.

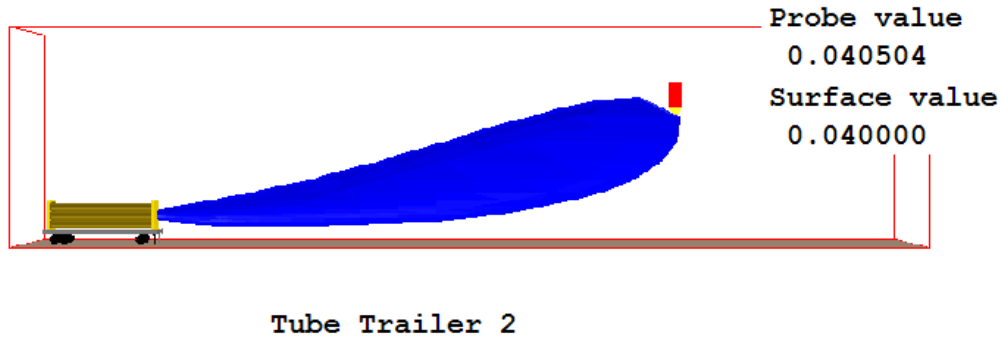


Figure 4. LFL (4% vol.) hydrogen cloud along the leak direction (Side view).

5.2. High Pressure Gas Storage Failure Scenarios

This section focuses on applying validated CFD models to simulate compressed hydrogen and methane release and dispersion from high-pressure gas storage tanks shown on Figure 5.



Figure 5. High-pressure hydrogen or CNG storage tanks

Compressed hydrogen (H_2) or methane (CH_4) is released from a set of storage tanks. The release orifice is 8.48 mm (1/2" OD).

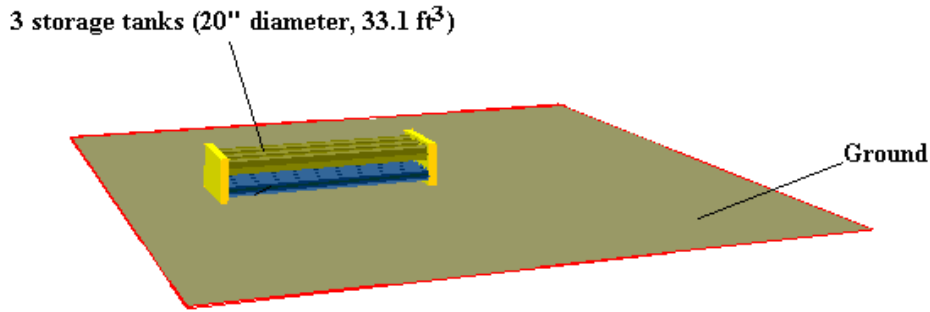


Figure 6. Storage geometry and domain for hydrogen and methane releases

3 big tanks (brown): OD 20", length 23'½", volume 33.1 ft³, pressure 4100 psi. The storage set is composed of three connected tanks, each of which has a diameter of 20" and a volume of 33.1 ft³. The total liquid volume for the storage is 99.3 ft³. The whole storage set has a length of 23'½" (7.023 m) and a height of 53'¾" (1.365 m). The working pressure is 4100 psi (284.4 bars) in each tank. The centerline of the storage tanks is in the middle of the domain and the wind in the domain is 0.5 m/s. The ambient temperature is 20 °C.

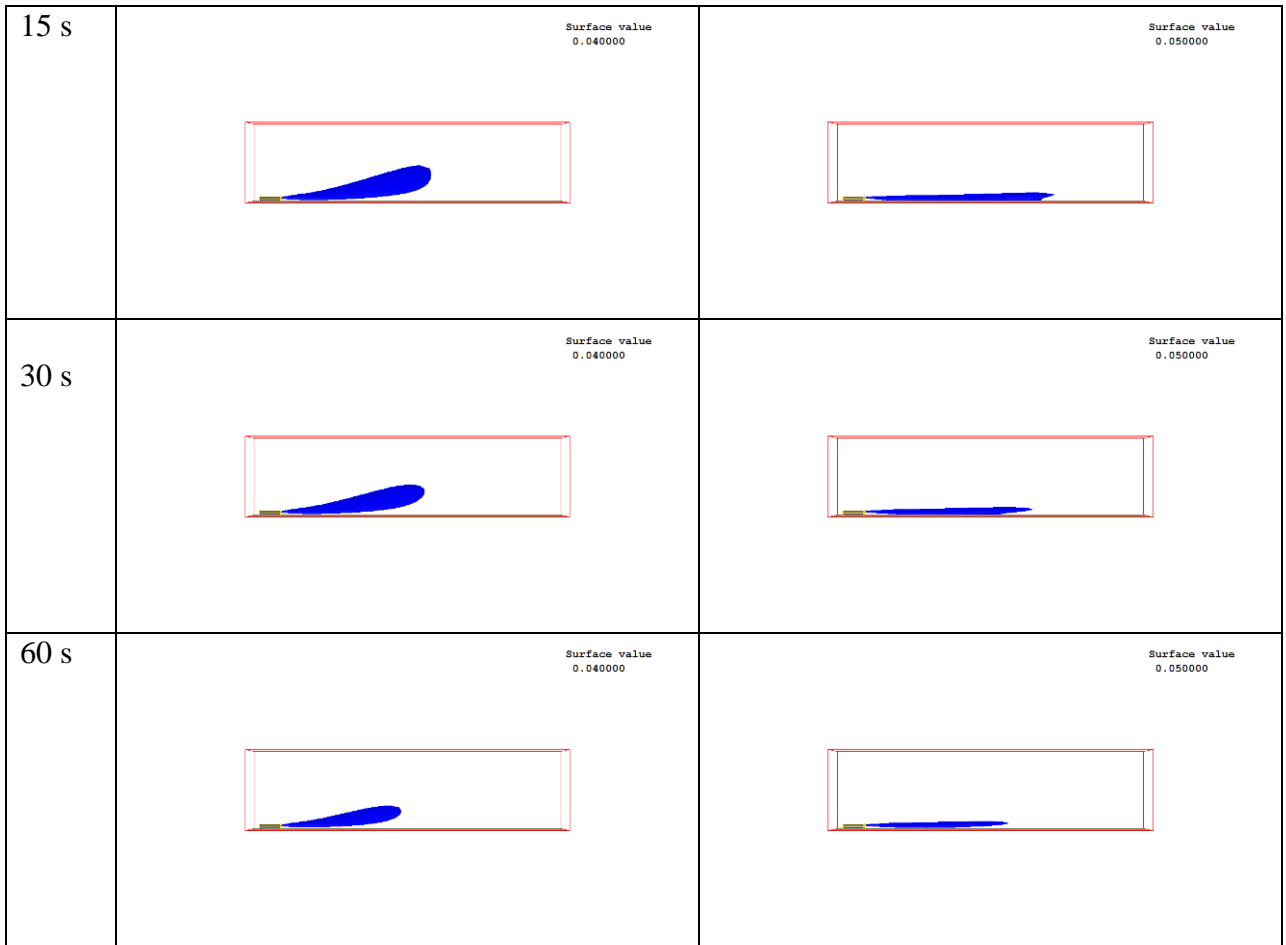
Numerical Results

Phoenics Simulations:

Table 4 shows the comparison of LFL clouds caused by the hydrogen and methane releases with time using the real-gas law, (the hydrogen release model was implemented by using the Abel-Noble real gas law and methane release was implemented using NIST real-gas properties. Note that Abel-Noble real gas law does not show consistency with methane under high pressure.) The LFL hydrogen cloud volume is larger than that of methane at each time and that the buoyancy force affects the hydrogen clouds much more than the methane clouds. The convection force prolongs the methane cloud in the leak direction more effectively than it does the hydrogen cloud.

Table 4 Comparison of transient hydrogen and methane releases using real gas law for both gases

Time	Hydrogen	Methane
5 s	<p>Surface value 0.040000</p> <p>The image shows a 3D simulation of a hydrogen release at 5 seconds. A blue, bell-shaped cloud is visible, rising from the ground level. The cloud is contained within a red rectangular box representing the simulation domain. The surface value of the cloud is 0.040000.</p>	<p>Surface value 0.050000</p> <p>The image shows a 3D simulation of a methane release at 5 seconds. A blue, elongated cloud is visible, rising from the ground level. The cloud is contained within a red rectangular box representing the simulation domain. The surface value of the cloud is 0.050000.</p>



Figures 7 and 8 show the transient hydrogen and methane cloud extents from the leak orifice for 60 seconds. The buoyancy forces substantially reduce the LFL cloud extent for hydrogen along the center line in comparison with the maximal cloud extent while. This phenomenon was not observed for methane.

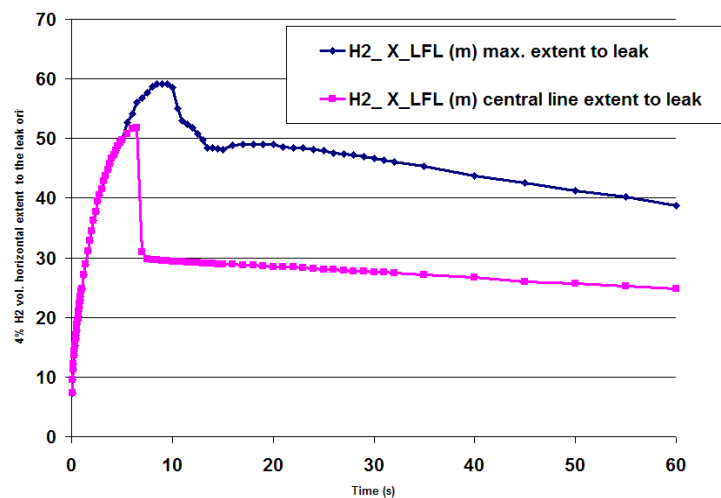


Figure 7. Hydrogen maximum and centerline cloud extents with time.

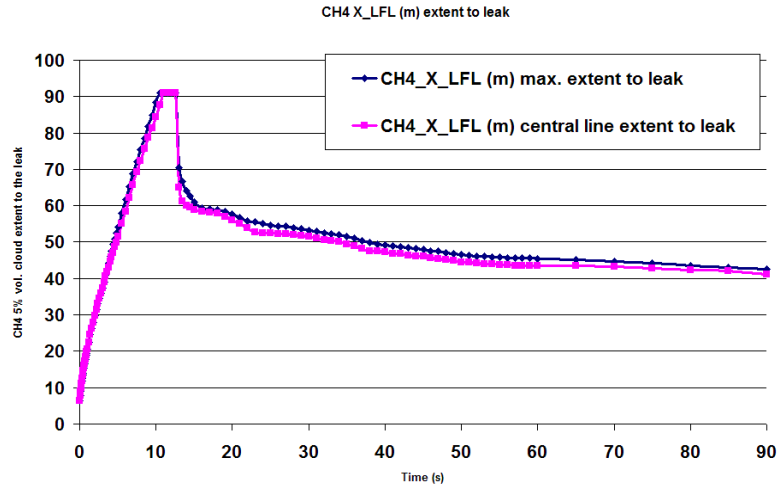


Figure 8. Methane maximum and centerline cloud extents with time.

Fluent Simulations:

Figures 9 and 10 show the results from Fluent simulations conducted for the same scenario for verification purposes. They show good qualitative agreement with Phoenics simulation results.

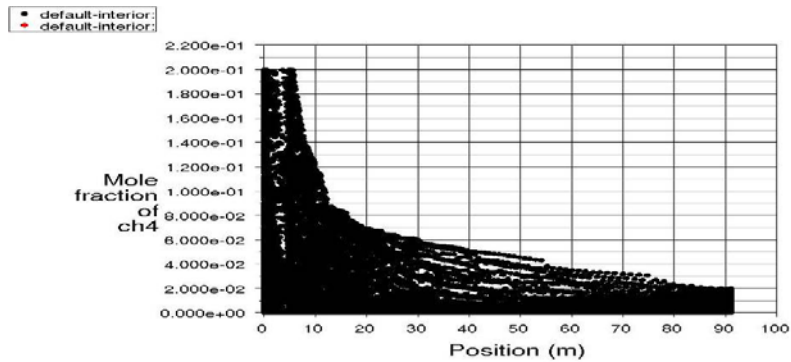


Figure 9. Methane horizontal cloud extent along the wind direction

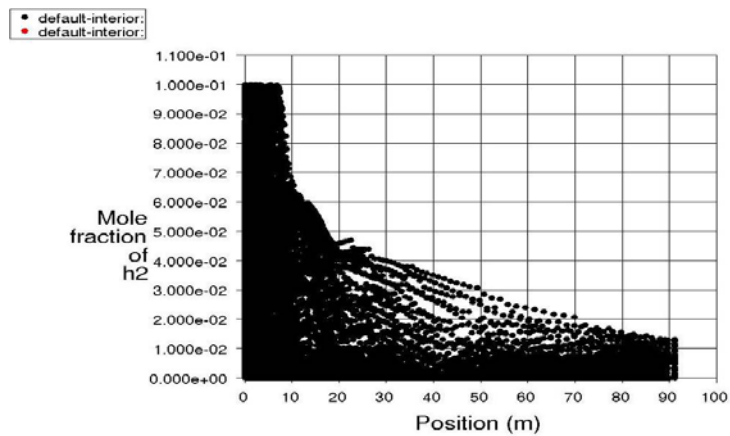


Figure 10. Hydrogen horizontal cloud extent along the wind direction

6. Probability Analysis

Probabilistic fault (FTA) and event (ETA) analyses provide a systematic and logical procedure to identify how system failures and sequences of failures can lead to the release scenarios and the likelihood of the end hazard or accident occurring. In this project the FaultTree+ program from Isograph Inc. was adopted for computation and display of the fault and event trees. The fault tree technique provides a method for evaluating the integrity of a system, particularly with regard to the ability of the system to survive the effects of minor failures of components without causing a hazardous condition. The fault tree analysis is a top-down method that has been used in almost all the fields to determine the frequency of the accident scenario. Potential accident outcomes and the general accident progression such as jet fire, flash fire, explosion or fireball for certain scenarios are then determined using the event tree analysis.

For the scenarios outlined in this report, probabilistic analysis first computed the likelihood of the Loss Of the Containment (LOC) scenarios occurring using a fault tree analysis (FTA). Pre-incident event trees then were used to further assess the effect of automatic system response and emergency operator actions which are the overall mitigating systems in place on the probability of post-release duration/or severity effects.

- *Failure of the hydrogen detection and automatic shutdown leading to Automation-Limited Release*
- *Failure of the hydrogen detection and manual shutdown leading to Manual-Limited Release*
- *Failure of both automated and human intervention systems leading to No Intervention-Unlimited Release*

6.1. Ignition Probabilities

Immediate ignition of hydrogen releases leads to different consequences than delayed ignition. Immediate ignition will lead to jet fires for continuous leaks and fireballs for rupture, whereas delayed ignition of a continuous or instantaneous leak leads to a flash fire or deflagration. Hence it is essential in the risk study to separately control both the immediate and the delayed ignition probability, which should be in line with historical ignition probability data.

The DNV database provides extensive historical ignition probability data. It also shows the reported ratio of immediate to delayed ignition probability historically is 2 to 1.

The data for hydrocarbons shows that probability of ignition for gas leaks lower than 1 kg/s is 0.01. The hydrogen leak rates in this study are also within this range.

Following the DNV guide line would imply that all hydrogen leaks would have to be modeled with an overall ignition probability of 1 percent.

However, for a given mass leak rate, hydrogen would form an 8 x larger flammable cloud than methane, as the cloud size this is determined by the flow in mole per second, rather than flow in kg/s. (8 x, as both hydrogen and methane have a similar lower flammable limit). It is obvious that for delayed ignition the ignition probability increases with increased flammable cloud size. Hence an argument may be made to

change the critical release rate for hydrogen by a factor 8; i.e. 1 kg/s for methane is equivalent to 0.125 kg/s for hydrogen, etc.

The flammable range of hydrogen is 4 to 75 volume percent, which is a factor 7.3 higher than for methane (5 to 15 volume percent). One may be inclined to think that this would significantly increase the likelihood of delayed ignition of hydrogen when compared to methane. However, this is contradicted by consequence modeling dispersion results for equal size clouds (i.e. for similar mole/s leak flow rates). For both methane and hydrogen, the size of a cloud above 15 mole percent is approximately 16% of the total size of cloud above LFL. Hence the larger flammable range of hydrogen does not materially affect the delayed ignition probability.

Given the very low minimum ignition energy for hydrogen (0.02 mJ, when close to stoichiometric mixture) as compared to methane (0.29 mJ), a 1 percent overall ignition probability for hydrogen leaks < 0.125 kg/s would seem to be too low, as hydrogen may be easily ignited by very weak ignition sources including static, which may be caused by line friction, build-up static on operator clothing, rotating machinery, or accidental uncoupling of a re-fuelling hose. This would justify increasing the hydrogen release ignition probability to be higher than the 1 percent suggested by DNV data.

An opposing argument is that the hydrogen ignition probability should be regarded as similar to methane, as at concentrations up to 10% vol. hydrogen would require similar ignition energy as methane.

Despite significant research, DNV has not been able to locate definitive data on historical hydrogen release ignition probabilities. Hence, based on the above discussion it was proposed to reasonably conservative approach:

- Reduce the leak flow ranges by a factor 8 for hydrogen, allowing for differential molecular weight as compared to methane, which directly affects the size of flammable cloud.
- Increase the gas ignition probabilities by 16 percent, allowing for the ratio of the flammable range of hydrogen compared to methane, and allowing that the 15 vol. % to 75 vol. % portion of any hydrogen cloud (due to pressurized releases) constitutes only 16 percent of the total cloud size above LFL.
- Treat the ignition probability of hydrogen as similar to methane, allowing that for most of the flammable cloud size is near the lower flammable range, where the minimum ignition energy required is similar to methane.
- Consider overall hydrogen ignition probability as 0.012 and immediate ignition probability as 0.008.

7. Consequence Analysis – Thermal Effects

In this study only immediate ignition thermal effects are analyzed.

Potential thermal effects resulting from the horizontal releases of hydrogen and methane (Scenarios 1 to 11) were simulated by using the correlations and model developed by Y. R. Sivathanu [3] and W. Houf [4]. This model assumes that a high-pressure leak of hydrogen or methane is ignited at the source can best be described as

a classic turbulent-jet flame. For turbulent-jet flames, the radiative heat flux at an axial position and radial position can be expressed in terms of the non-dimensional radiant power and total emitted radiative power. The approach is validated by the reported experimental measurements of large-scale hydrogen jet flames. The experiments verified that measurements of flame length, flame width, radiative heat flux, and radiant fraction are in agreement with non-dimensional flame correlations reported in the literature. The current work exploits such correlations to predict the radiative heat flux from a wide variety of hydrogen and methane flames (Scenarios 1 to 11).

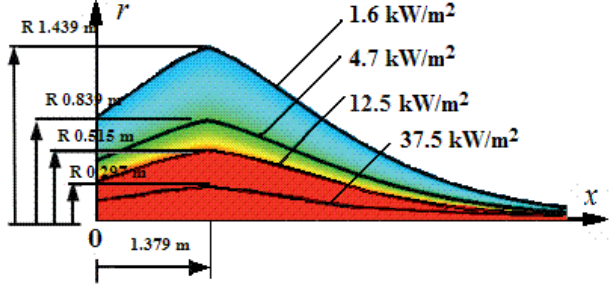
The thermal fluxes emitted by methane or hydrogen vertical flares (Scenario 12) were calculated based on fixed volumetric flow rate by assuming a 9 m/sec crosswind towards a vertical target surface area. The differences between hydrogen and methane flares mainly stem from their different densities and heat of combustions. The net heat release is proportional to the gravimetric heat of combustion multiplied by the density. At fixed volumetric flow rate, the heat release of methane is 2.8 times larger than hydrogen. The model also predicts somewhat longer and broader flames for methane. The Shell-Research at Thornton model (Chamberlain, 1987) was used to calculate the properties of the flame and the thermal flux from the venting of hydrogen and natural gas at 2000 SCFM (Scenario 12). The model has been validated for natural gas and is considered reliable for hydrocarbon gases. We should note that this model is usually applied to large scale flares (the TNO [4] example is for a 30 kg/second outflow). It predicts shorter flame lengths for flares in the presence of a crosswind.

Below, as a representative example, is the description of thermal effects that could potentially be produced by modeled failure scenarios for tube trailer and storage. Each scenario is addressed via a table that contains a diagram with distances to selected thermal threshold levels. The diagrams show maximum values for each threshold level in radial direction, i.e. outside the jet flame. Because of different intensity of releases in selected scenarios, the maximum values are achieved at different axial distances from the point of release. In order to compare thermal effects at equal distances from the points of release and resulting jet fires, the tables also contain the numbers for locations 1 m and 5 m away from the point of release in axial direction and 1 m in radial direction. They are marked $(x, R) = (1 \text{ m}, 1 \text{ m})$ and $(x, R) = (5 \text{ m}, 1 \text{ m})$ respectively. The values of thermal effects at these locations are used for risk calculations in Risk Estimation section below. For cases when selected locations are within the flame (and thermal effects thus exceed 37.5 kW/m^2), the fatality probability is considered to be equal to 1.

7.1. Tube Trailer – Scenario 1

Small size leak (1 mm) on a ½” pipe line during unloading. Pressure – 2640 psig. leak direction – horizontal; type of release – sonic jet. Mode of release – steady state, constant flow.

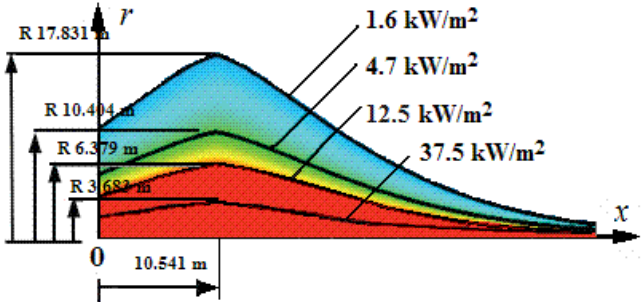
Table 5 Thermal effects for tube trailer – Scenario 1

<p>Diagram</p>	<p>Radiative heat fluxes for hydrogen jet flame</p> <p>Inside high-pressure tank: Stagnation pressure: 182 bars Stagnation temperature: 293.15 K Leak orifice diameter: 1 mm Visible flame length: 2.172 m Visible flame width 0.369 m</p> 
<p>Thermal flux at (x, R) = (1.0 m, 1.0 m) (kW/m²)</p>	<p>3.0</p>
<p>Thermal flux at (x, R) = (5.0 m, 1.0 m) (kW/m²)</p>	<p>0.0</p>

7.2. Tube Trailer – Scenario 2

Catastrophic failure hydrogen release from ½” pipe line during unloading. Mode of release –steady state, constant flow.

Table 6 Thermal effects for tube trailer – Scenario 2

<p>Diagram</p>	<p>Radiative heat fluxes for hydrogen jet flame</p> <p>Inside high-pressure tank: Stagnation pressure: 182 bars Stagnation temperature: 293.15 K Leak orifice diameter: 8.48 mm Visible flame length: 16.6 m Visible flame width 2.822 m</p> 
<p>Thermal flux at (x, R) = (1.0 m, 1.0 m) (kW/m²)</p>	<p>Location within the flame. Thermal effects are much greater than 37.5 kW/m². Fatality.</p>
<p>Thermal flux at (x, R) = (5.0 m, 1.0 m) (kW/m²)</p>	<p>Location within the flame. Thermal effects are much greater than 37.5 kW/m². Fatality.</p>

7.3. Hydrogen and Methane Gas Storage – Scenario 11

Hydrogen and CNG similar type leaks through a 8.48 mm orifices from a 3 cylinder bank at 4100 psig. Leaks are sonic and horizontal.

Table 7 Thermal effects for methane gas storage

<p>Diagram</p>	<p>Radiative heat flux for methane jet flame</p> <p>Inside high-pressure tank: Stagnation pressure: 282.6 bars Stagnation temperature: 293.15 K Leak orifice diameter: 8.48 mm Visible flame length: 23.458 m Visible flame width 3.988 m</p>
<p>Thermal flux at (x, R) = (1.0 m, 1.0 m) (kW/m²)</p>	<p>Location within the flame. Thermal effects are much greater than 37.5 kW/m². Fatality.</p>
<p>Thermal flux at (x, R) = (5.0 m, 1.0 m) (kW/m²)</p>	<p>Location within the flame. Thermal effects are much greater than 37.5 kW/m². Fatality.</p>

Table 8 Thermal effects for hydrogen gas storage

<p>Diagram</p>	<p>Radiative heat fluxes for hydrogen jet flame</p> <p>Inside high-pressure tank: Stagnation pressure: 282.6 bars Stagnation temperature: 293.15 K Leak orifice diameter: 8.48 mm Visible flame length: 20.82 m Visible flame width 3.539 m</p>
<p>Thermal flux at (x, R) = (1.0 m, 1.0 m) (kW/m²)</p>	<p>Location within the flame. Thermal effects are much greater than 37.5 kW/m². Fatality.</p>
<p>Thermal flux at (x, R) = (5.0 m, 1.0 m) (kW/m²)</p>	<p>Location within the flame. Thermal effects are much greater than 37.5 kW/m². Fatality.</p>

7.4. Hydrogen and Methane Gas Storage Venting – Scenario 12

Venting of hydrogen and CNG through the same vent stack at 2,000 CFM flow rate.
Type – sonic and subsonic; mode – steady state.

Table 9 Comparative thermal effects for hydrogen methane gas storage venting

Model	TNO Yellow Book			
Gas Storage	Scenario 12			
Gas Type	Natural Gas		Hydrogen	
Nature of the outflow	Sonic	Subsonic	Sonic	Subsonic
Flow rate, m ³ /sec	0.94	0.94	0.94	0.94
Mass flow rate kg/s	0.63	0.63	0.08	0.08
Stack height (m)	3.66	3.66	3.66	3.66
Stack diameter (cm)	2.5	7.5	2.5	5.0
Net flame length (m)	4.50	6.64	2.56	3.32
Min flame diameter (m)	0.35	0.46	0.07	0.15
Max flame diameter (m)	1.68	2.91	0.83	1.30
Lift-off height (m)	0.88	0.69	0.52	0.54
Tilt angle (degrees)	31.43	56.97	19.88	32
Max rad. flux at Human Height (kW/m ²)	10.64	21.66	4.97	6.93
Distance to maximum flux (m)	2.71	2.97	2.10	2.18
Distance to 1.6 kW/m ² (m)	14.92	19.08	7.88	9.69
Distance to 4.7 kW/m ² (m)	8.23	12.39	1.48	3.63
Distance to 12.5 kW/m ² (m)	N/A	7.53	N/A	N/A
Distance to 37.5 kW/m ² (m)	N/A	N/A	N/A	N/A

8. Risk Metrics and Risk Estimation

Metrics were adopted to quantify the individual and societal risks associated with the scenarios analyzed in this project to effect comparisons between selected hydrogen sourcing, storage and hydrogen production components in hydrogen refuelling options. These were computed using HyQuantras™, a computerized toolkit for quantifying the risk associated with the jet-fire scenarios used for these comparisons.

HyQuantras™ computes the risk as individual and societal risk measures

- Location-Specific Individual Risk (LSIR)
- Individual-Specific (ISIR)
- Potential Loss of Life (PLL)
- Expected Number of Fatalities (ENF)

Of these, the LSIR and PLL were used for the project comparisons.

While individual risk is based upon the risk at a specific location, the societal risk (SR) indicates how many people can be involved in an accident simultaneously and is related to defined population that could be affected, usually in terms of injury or

fatality. Societal risk gives an indication of the risk of an industrial activity in a specific populated environment; hence societal risk depends upon both the type and magnitude of the release activity and the distribution of the surrounding population. It is often expressed as the likelihood of specified number of fatalities or the expected number of fatalities per unit of time, for example, the potential loss of life (PLL) associated with a facility that is given by:

$$PLL = LSIR \times n_{\text{present}}$$

where n_{present} is the number of persons present and exposed to the event.

Exposure times of 20 seconds and one-minute (60 seconds) exposure time were selected for the analysis with exceptions of shorter times for release scenarios in electrolyser and reformer enclosures. The Probit equation used in this analysis is that given for outdoors (or for unprotected people) in the TNO “Purple Book” Guidelines for Quantitative Risk Assessment [5]. The number of people exposed to the hazard was considered as 4.

8.1. Examples of Risk Estimation

Below are examples of risk estimation for tube trailer failure scenarios.

Tube trailer data are available from Scenarios 1 and 2 analyses that describe small and large releases, respectively, during unloading. In Table 10 for Scenario 1, there is no significant risk due to an insufficient dose-response because, being a small leak through a 1 mm² effective orifice, the quantity of hydrogen does not produce significant heat radiation and, secondly, because at the selected exposure times of 20 and 60 seconds there is no significant harm to an individual located at the points (x, R) = 1,1 and (x, R) = 5.1.

Table 10 Scenario 1: Small leak from a tube trailer

Scenario Name	Scenario 1			
Scenarios Description	Small Leak from Tube Trailer during Unloading			
	Location			
Frequency	4.20E-05		1,1	
Thermal Consequences	3		Risk OnsetThreshold	
Exposure Time	20 60		100 20 60	
LSIR	No Risk - Insufficient dose response		5.00E-07 No Risk - Thermal Intensity is less than ambient	
PLL	No Risk - Insufficient dose response		2.50E-06 No Risk - Thermal Intensity is less than ambient	

However, the Onset Threshold column shows that, at the heat radiation level of 3 kW/m² for the closest location (x, R)=1.1 an average exposure of 100 seconds would account for 1% lethality among the people exposed to it at the LSIR and PLL values shown in the table.

Table 11 Scenario 2: Large leak from a tube trailer

Scenario Name	Scenario 2							
Scenarios Description	Large Leak from Tube Trailer during Unloading							
		Location						
						Distance for 12.5	Distance for 4.7	
Frequency	2.50E-06	1,1		5,1		threshold = 10.5,6.4	threshold = 10.5,10.4	
Thermal Consequences	37.5		37.5		12.5		4.7	
Exposure Time	20	60	20	60	60		60	
LSIR	2.50E-06	2.50E-06	2.50E-06	2.50E-06	2.30E-06		5.20E-08	
PLL	1.00E-05	1.00E-05	1.00E-05	1.00E-05	9.20E-06		2.10E-07	

In Table 11 for Scenario 2 representing a large hydrogen leak, due to the large amount of hydrogen released the thermal load received by an individual at the two considered locations, that in this case are inside the flame, is very large and exceeds 37.5 kW/m² producing to 100 % lethality for the selected exposure times of 20 and 60 seconds. At further distances from these reference locations, 12.5 and 4.7 kW/m² heat load impacts yield 92 % lethality at (x,R) = 10.5,6.4 and 2 % lethality (x,R) = 10.5, 10.4 for people exposed to those values. The LSIR values corresponding to 100 % lethality for the first and second locations equal the frequency of the end outcome. The LSIR for 12.5 kW/m² for the third location indicating a value of 92 % lethality is very close to that of the reference distances. At the threshold level of 4.7 kW/m² there is a 2 % lethality for the people happen to be there.

9. Conclusions

Producing hydrogen on-site by electrolysis presents a lower individual and societal risk than producing hydrogen on-site by steam methane reforming, presumably because the complexity of the installation in the SMR case and also because in the SMR there are the both gases present. Sourcing hydrogen on-site and off-site present almost the same risk. From the individual risk, the electrolysis process presents the lower risk, followed by tube trailer and the third with highest risk for the reformer.

A comparison of the relative risk associated with hydrogen and natural gas storage shows that hydrogen storage facility presents a marginally lower (within 20%) risk compared to an identical CNG storage in regards to accidental horizontal-jet release from storage connecting piping. In terms of storage venting, a CNG storage facility may require either a larger clearance than an identical hydrogen storage facility or a higher vent stack to achieve the same level of thermal radiation from a vertical flare.

In summary, an electrolysis refuelling option that includes compressed hydrogen storage presents the lowest risk among the refuelling options that were considered including a CNG station of equal refuelling capacity to provide equivalent travel mileage.

10. Acknowledgments

Partner Input

A.V.Tchouvelev & Associates Inc., the Hydrogen Research Institute and TISEC Inc. carried out the project. Input from the following partnering companies/individuals helped establish a baseline for comparative modeling scenarios addressed in the project and interpretation of results:

- TIAX
- Marsh
- FM Global

Financial Support

Support for the project was provided by Natural Resources Canada through the activities of the Codes and Standards Working Group of the Canadian Transportation Fuel Cell Alliance, by the research performers, A.V.Tchouvelev & Associates Inc., TISEC Inc., and the Hydrogen Research Institute, and by the collaborating industrial partners.

Special Thanks

Special thanks to Stefan Unnasch from TIAX for very useful and valuable discussions regarding comparative scenarios of hydrogen refuelling options as well as CNG refuelling station baseline, and for the permission to use TIAX report to the California Energy Commission “Failure Modes and Effects Analysis of Hydrogen Fueling Options” CEC-600-2005-001.

11. References

1. CTFCA *Comparative Quantitative Risk Estimation of Hydrogen and CNG Refuelling Options*, A.V.Tchouvelev, D.R. Hay, P. Benard et al, Final Report, March 2006.
2. TIAX “Failure Modes and Effects Analysis of Hydrogen Fueling Options” CEC-600-2005-001, January 2005.
3. Y. R. Sivathanu and J. P. Gore, *Total Radiative Heat Loss in Jet Flames from Single Point Radiative Flux Measurements*, Combustion and Flame 94: 265-270 (1993)
4. W. Houf and R. Schefer, *Predicting Radiative Heat Fluxes and Flammability Envelopes from Unintended Releases of Hydrogen*, International Journal for Hydrogen Energy, 2006.
5. TNO “Yellow Book” *Methods for the calculation of physical effects*, Committee for the prevention of disasters, Part 2, p.6.48, 1997.
6. TNO “Purple Book” *Guidelines for Quantitative Risk Assessment*, CPR 18E, Committee for the prevention of disasters, First edition, 1999.